

Non-linear piezoelectricity in zinc blende GaAs and InAs semiconductors

G. Tse, J. Pal, U. Monteverde, R. Garg, V. Haxha et al.

Citation: *J. Appl. Phys.* **114**, 073515 (2013); doi: 10.1063/1.4818798

View online: <http://dx.doi.org/10.1063/1.4818798>

View Table of Contents: <http://jap.aip.org/resource/1/JAPIAU/v114/i7>

Published by the AIP Publishing LLC.

Additional information on J. Appl. Phys.

Journal Homepage: <http://jap.aip.org/>

Journal Information: http://jap.aip.org/about/about_the_journal

Top downloads: http://jap.aip.org/features/most_downloaded

Information for Authors: <http://jap.aip.org/authors>

ADVERTISEMENT



AIPAdvances

Now Indexed in
Thomson Reuters
Databases

Explore AIP's open access journal:

- Rapid publication
- Article-level metrics
- Post-publication rating and commenting

Non-linear piezoelectricity in zinc blende GaAs and InAs semiconductors

G. Tse,¹ J. Pal,¹ U. Monteverde,¹ R. Garg,¹ V. Haxha,¹ M. A. Migliorato,¹ and S. Tomić²

¹*School of Electrical and Electronic Engineering, University of Manchester, Manchester, United Kingdom*

²*Joule Physics Laboratory, School of Computing, Sciences and Engineering, University of Salford, Salford, United Kingdom*

(Received 6 March 2013; accepted 2 August 2013; published online 21 August 2013)

This work explores the strain dependence of the piezoelectric effect in GaAs and InAs zinc blende crystals. We write the polarization in terms of the internal anion-cation displacement and the ionic and dipole charges. We then use *ab initio* density functional theory to evaluate the dependence of all quantities on the strain tensor. We investigate which aspects of the elastic and dielectric response of zinc blende crystals are sources of non-linearities in the piezoelectric effect. We observe that the main source of non-linearities is the response to elastic deformation and, in particular, the internal sublattice displacement of the interpenetrating cation and anion sublattices. We show that the internal sublattice displacement dependence on the diagonal stress components is neither symmetric nor antisymmetric in the strain. Therefore, non-linear coefficients of order higher than quadratic are needed to correctly describe non-linear effects. Using a fitting procedure of the *ab initio* data, we also determine all non-linear piezoelectric coefficients up to the third power in the diagonal components of the strain tensor. We can report that non-linear effects up to third order can be significant in precisely determining the magnitude of the piezoelectric polarization if compressive or tensile strains larger than 10% are present. We notice however that, in nanostructures such as quantum dots, the optical properties are less sensitive to the third order non-linear piezoelectric effect and that third order coefficients can therefore be neglected. © 2013 AIP Publishing LLC. [<http://dx.doi.org/10.1063/1.4818798>]

I. INTRODUCTION

The piezoelectric (PZ) effect in bulk III-V semiconductors arises from lack of inversion symmetry along one or more particular crystallographic directions known as polar axes.^{1,2} PZ effects are found in devices as diverse as light-emitting diodes (LEDs), lasers, power devices, transducers, and micropositioners.³ Furthermore, the recently discovered field of Piezotronics⁴⁻⁷ has highlighted the potential for exploiting the PZ field in nanostructured semiconductors for the realization of self-powering devices, nanogenerators, pressure sensors, and in flexible electronics applications.

In III-V semiconductors, strain with a component along the polar axis of the crystal leads to the generation of electrical dipoles. In zinc blende (ZB) crystals, such dipoles are created in response to shear strain, i.e., the off-diagonal components of the strain tensor and manifest themselves as a macroscopic PZ field that exists, for instance, in quantum wells (QWs) grown on [111] oriented substrates, quantum wires, and quantum dots (QDs). A similar effect is also observed in wurtzite (WZ) semiconductors along the polar axis [0001] when the crystal is deformed by either parallel or perpendicular strain, i.e., the diagonal components of the strain tensor.

Though the piezoelectric field in semiconductors has for a long time been treated as a linear effect in the strain, the influence of non-linearities has been highlighted in WZ III-N,⁸ ZB II-VI,^{9,10} and ZB III-V^{11,12,15} semiconductors.

All previous studies concur on the importance and of non-linear effects and their magnitude.^{11,12} It is also generally acknowledged⁹ that the two most widely used methods

employed to evaluate such effects, namely, the linear response method (LRM)¹³ and Harrison's method (HM),¹⁴ appear to produce different results. In order to shed some light into this discrepancy, one needs to compare directly the coefficients predicted by the two methods. This has not yet been achieved because data obtained using HM^{11,15} were so far given as an incomplete set, i.e., a subset of the dependence upon the full strain tensor. In this paper, we in part address this issue and present the piezoelectric coefficients (PZCs) dependence on all combinations of the diagonal components of the strain tensor. The reason that is difficult to fully address the issue of comparing the two models is that for a full comparison involving also the shear components HM^{11,15} would involve an unfeasible number of simulations to completely map the dependence on all strain components, as it will be discussed in detail in Sec. III.

II. METHODOLOGY

The method we have previously developed¹¹ is based on a semi-empirical approach, where the piezoelectric charges are given by the sum of a direct dipole contribution and a bond contribution, as originally proposed by Harrison.¹⁴

In order to evaluate all the linear and non-linear coefficients, we determined the total strain induced polarization using the framework validated on experimental data from InGaAs QWs^{11,15}

$$P_{\hat{x}_i} = \frac{Z_H^* \delta \mathbf{x}_i + 2\alpha_p (1 - \alpha_p^2) \cdot \sum_{q=1}^4 (\vec{r}_q \cdot \hat{x}_i) \delta R_q}{2\Omega}, \quad (1)$$

where \hat{x}_i is the Cartesian direction, $\delta\mathbf{x}_i$ is the displacement vector of cations with respect to anions from the ideal position, r_q and $\delta\mathbf{R}_q$ are the distance and displacement vectors of the nearest neighbour q from the atom at the centre of the tetrahedron, α_p is the bond polarity, and Ω is the atomic volume. Borrowing from the language of tight binding, Z_H^* is the atomic charge, generally different from the transverse effective charge, which instead has its direct equivalent in the dynamic effective charge or Born charge (Z).

In our previous work,^{8,11,15} we have demonstrated that Z_H^* is always a fraction of the value of the dynamic effective charge (Z^*), if the values of the PZ polarization are to be in agreement with experiment. In fact, in III-N materials, calculating the PZCs by using Z^* leads to grossly overestimated strain induced PZ fields, as confirmed by Bernardini and Fiorentini.¹⁶

The effective charge was used in our model to evaluate the bond polarity

$$Z^* = -\Delta Z + 4\alpha_p + 4\alpha_p(1 - \alpha_p^2), \quad (2)$$

where $\Delta Z = 1$. The atomic charge Z_H^* in our model is always determined, so that once α_p and the elastic deformation have been calculated in the limit of small strain (Bulk crystals), the model correctly reproduces experimental values of the PZC.

For both bulk and strained cases, the elastic deformation and Z^* were evaluated by using plane wave pseudopotential (with pseudopotentials derived with the Troullier–Martin scheme¹⁷) density functional theory in the local density approximation (DFT-LDA)¹⁸ and density functional perturbation theory (DFPT) within the CASTEP¹⁹ code.

Such choice is based on our own experience and the fact that, e.g., the generalized gradient approximation appears not to work as well as LDA for problems involving structural relaxation of semiconductor materials.²⁰

III. DFT CALCULATIONS: INTERNAL DISTORTION

The first important quantity needed in the evaluation of Eq. (1) is the Kleinman parameter of internal distortion.²¹ We used a strain tensor of the form:

$$S = \begin{pmatrix} 1 + \varepsilon_1 & \gamma/2 & \gamma/2 \\ \gamma/2 & 1 + \varepsilon_2 & \gamma/2 \\ \gamma/2 & \gamma/2 & 1 + \varepsilon_3 \end{pmatrix}, \quad (3)$$

where reduced indexes ($x = 1$, $y = 2$, $z = 3$, $yz = 4$, $xz = 5$, $xy = 6$) are used.

We note that the strain tensor in Eq. (3) is not completely generalized, as the off diagonal components (shear strain) are taken to be identical. In this case, the displacement is purely uniaxial. This particular form of the strain tensor was chosen to limit to 3 in the dimensionality of the problem, when a fixed small value of γ is used and ε_1 , ε_2 , and ε_3 are varied independently.

Even with such a reduced dimensionality, we require roughly 10^3 DFT calculations for each material investigated. If we also varied γ , we would require a total of 10^4 calculations,

surging to 10^6 if independent shear strains were also included. Going beyond, 10^3 independent calculations is impractical, particularly, when one takes into account the difficulty in achieving convergence of all DFT simulations, as much as possible without changing conditions, such as the number of K points or energy cut-off between simulations. On a few occasions, more stringent convergence criteria had to be applied especially for data points calculated under the condition of very high strain. Since for each set of convergence criteria the relaxed lattice parameter changes, altering these parameters makes comparison between different DFT simulations extremely difficult. We therefore tried to minimize the need for changing convergence criteria. To ensure that data points were correctly converged, we found it very helpful to perform graphic checks of the data and therefore be able to pick out visually those data points that did not appear to be respecting the trend given by the other data points. This would have also become challenging, if the full dependence on all the components of the strain tensor had been investigated.

The less computationally demanding LRM used by Beya-Wakata *et al.*¹³ can easily consider 3 independent off diagonal (shear) strain components together with 3 independent diagonal components, therefore, using the full strain tensor.

Given that in our calculations such generalization is instead computationally demanding, we restrict our investigation to the non-linear behaviour in the diagonal components, in the limit of small shear strain. Such approach can be justified in the following way. First, we notice that in Migliorato *et al.*¹¹ the Kleinman parameter has a weak dependence on shear strain (e.g., from 0.45 to 0.40 in GaAs), for values of $\gamma < 0.05$, which is roughly the largest values of the shear strain normally encountered in nanostructures. Second, a large dependence was instead recorded upon the diagonal strain components: for hydrostatic strain between 0 and 0.1, the Kleinman parameter of GaAs varies from 0.45 to 0.80. Third, the dependence on the non-linear shear strain was predicted to be very small also in the LRM calculations of Beya-Wakata *et al.*¹³ Fourth, we will show in Sec. VI that the dependence on the diagonal strain components can be fitted by a cubic equations, where the small non-linear shear strain dependence is contained in the noise of both the DFT calculations and the fitting procedure. The contribution from non-linear shear strain would therefore be difficult to distinguish as it would always be overshadowed by the much larger dependence on the diagonal strain components. In conclusion, the approach of neglecting the non-linear dependence on the shear strain does not detract in any way from the validity of the present calculations in the limit of small strain, while representing only a marginal correction to the case of large shear strain, as already shown in our previous work.¹¹

The Kleinman parameter is linked to the overall cation-anion displacement Cartesian components through the relationship

$$d\hat{x}_i = \frac{\zeta_{\hat{x}_i} \gamma a}{4(1 + \varepsilon_{\hat{x}_i \hat{x}_i})}. \quad (4)$$

This equation is our own revision of the original definition given by Leonard Kleinman.²¹ Such revised form is necessary

because the parameter was originally defined to be a material constant whereas in our description is treated as a 3 dimensional vector function of the strain, as already described in Garg *et al.*¹⁵ Furthermore, we prefer to use explicitly the strain components in the definition to preserve the original physical meaning of the parameter, i.e., a value of 1 maintains all bond angles equal to each other irrespective of the amount of shear strain applied to the crystal.

IV. DFT CALCULATIONS: BOND POLARITY

The bond polarity is obtained from calculations of the effective charges from DFPT with the Berry phase approach.²² Energy Cut-Off of 3000 eV and MP K-Point grid of $6 \times 6 \times 6$ provided a convergence error of less than 0.01%. For InAs, 2000 eV and $8 \times 8 \times 8$, a convergence error of less than 0.001% was obtained. The Density Functional used in these calculations is the well-known Local Density Approximations (DFPT-LDA) with norm-conserving pseudopotentials.

The strain tensor used in these calculations is in the simple form of

$$S = \begin{pmatrix} 1 + \varepsilon_1 & 0 & 0 \\ 0 & 1 + \varepsilon_2 & 0 \\ 0 & 0 & 1 + \varepsilon_3 \end{pmatrix}, \quad (5)$$

as dependence on the shear strain is not necessary in this case. This approximation was tested, and at least for small values of the shear strain, was found to be valid. Furthermore, including a non-linear dependence on the shear strain makes it difficult to identify the charges components along the Cartesian axes, while also making the numbers of simulations required very large, as discussed earlier. Additionally, we note that the previous work^{11,15} demonstrated that non-linearities in the Kleinman parameter have a larger effect on the PZCs, compared with non-linearities in the bond polarity. Therefore, neglecting the shear strain dependence and only retaining the much larger dependence on the diagonal strain is always a reasonable approximation.

The calculation yields the Born Charges matrix, which when diagonalized results in 6 eigenvalues, λ_1 , λ_2 , and λ_3 for cations and λ_4 , λ_5 , and λ_6 for anions, respectively. The Born Effective Charge parameter Z^* is evaluated by averaging the 3 values

$$Z_{cation}^* = \frac{1}{3}(\lambda_1 + \lambda_2 + \lambda_3); \quad Z_{anion}^* = \frac{1}{3}(\lambda_4 + \lambda_5 + \lambda_6). \quad (6)$$

We then perform a further averaging

$$Z^* = \frac{1}{2} (|Z_{anion}^*| + |Z_{cation}^*|). \quad (7)$$

We relate the bond polarity to the effective charges through Eq. (2). The equation is cubic but yields only one physical solution, so that there is a unique correspondence of values of Z^* and α_p . For bulk GaAs and InAs, we obtain values of

α_p of 0.420 and 0.474, respectively, which is similar to previous calculations.^{11,15}

V. PIEZOELECTRIC COEFFICIENTS

The Kleinman vector and bond polarity data²³ are easily combined using Eq. (1), the only difficulty being the calculation of the geometrical factor that multiplies the bond polarity. This requires combining the strained positions of all the atoms in the tetrahedron under consideration, obtained in the DFT calculations of the internal distortion.

The calculated PZCs values are presented in Figs. 1–6, where the three coefficients e_{14} , e_{25} , and e_{36} are separated for ease of representation. These plots display the dependence in the strain components ε_1 and ε_2 for a value of ε_3 which increases in steps of 0.02 from -0.1 in the top left plot to $+0.1$ in the bottom right plot. The increase in ε_1 is left to right first and then onto the lower row. Not all possible combinations of diagonal strains are shown as cubic symmetry implies invariance upon exchange of ε_1 , ε_2 , and ε_3 . This obviously results in progressively less data points included in each sequence of plots for each figure.

The PZCs for both GaAs and InAs exhibit a similar behaviour as a function of strain and strong non-linear effects are present. It is important to note at this point that the linear model treats the PZC of zincblende as an isotropic material constant. Therefore, the fact that multiple values, both positive and negative, are predicted, depending on the applied strain, is already indicative of non-linear behaviour. Furthermore, the fact that the points are not equally spaced is also indicative that the PZCs depend super-linearly on the strain, while also differing in absolute value for tensile and compressive strain of equal magnitude. This is a clear indication of the absence of inversion antisymmetry $\varepsilon_i \leftrightarrow -\varepsilon_i$. In other words, compressive and tensile strain do not simply produce opposite results. This is to be expected, since crystals tend to resist compression more than they oppose expansion, an asymmetry which is obvious when one considers the cohesive energy diagrams of semiconductor materials.²⁴

Compared with the LRM, our model is therefore more complete as it yields the dependence on the diagonal strain components. By contrast in the LRM, both linear dependence on the diagonal strain terms and inversion antisymmetry are implicitly assumed by the choosing to only determine piezoelectric coefficients coupled to either $\varepsilon_1\varepsilon_2$, $\varepsilon_1\varepsilon_4$, $\varepsilon_4\varepsilon_5$, and their cyclic permutations.

The non-linear behaviour appears stronger in InAs compared with GaAs, as the curvature of the data for any constant value of ε_2 is more noticeable in the former compared with the latter. This is the direct result of the difference in the Kleinman deformations as a function of strain, which can be seen in the Supplementary Material.

In our model, compared with the LRM, the existence of both positive and negative values of the PZCs can be explained in a physical way. In fact, the sign of the coefficient depends on the relative magnitude of the two terms in Eq. (1). Since the signs of the two terms are opposite, the first term (direct dipole contribution) tends to dominate for low strain and provide an overall negative sign. On the other

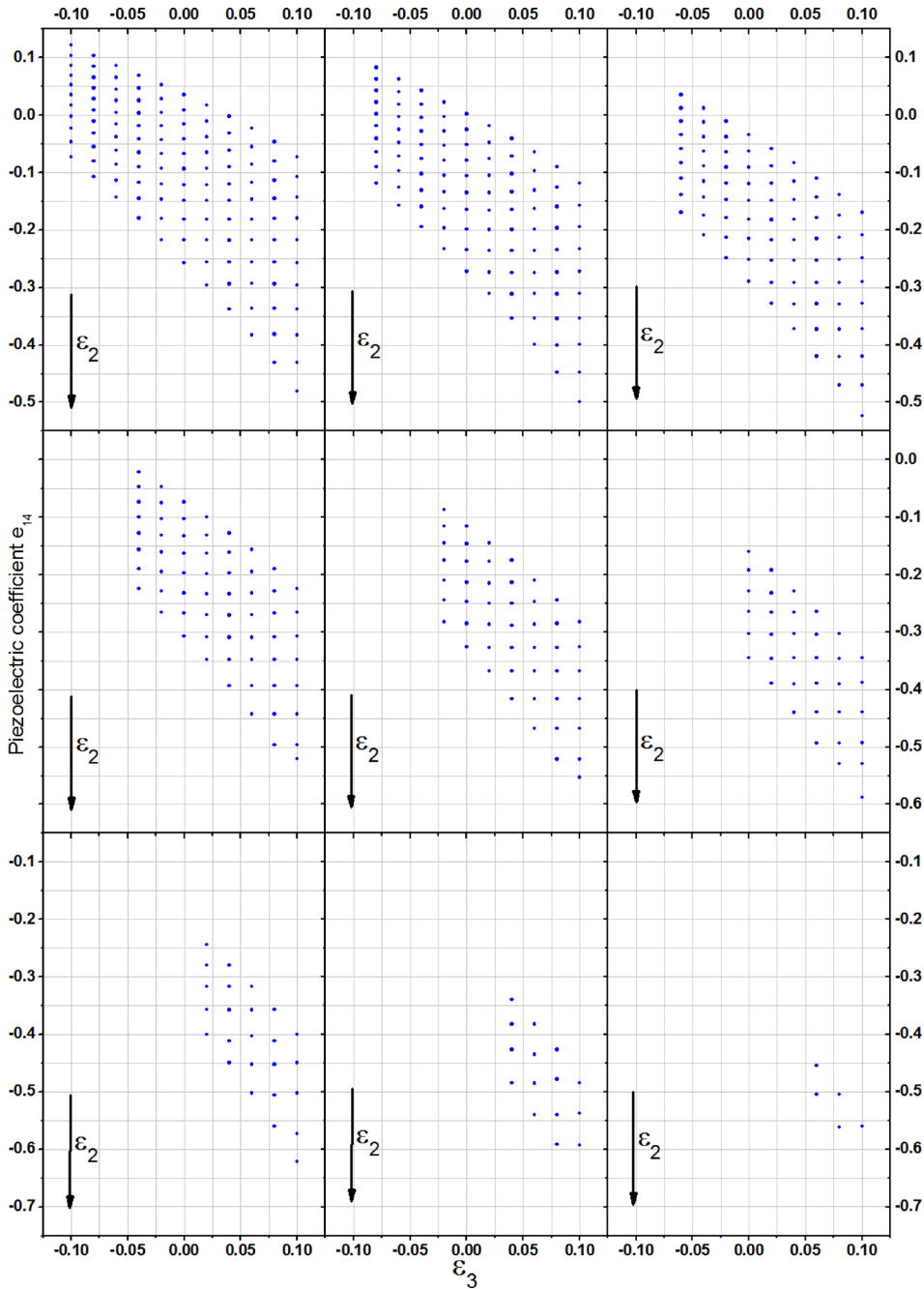


FIG. 1. Piezoelectric coefficient e_{14} (C/m^2) dependence on strain for GaAs calculated from *ab-initio* DFT. The data display the dependence upon the strain components ε_1 and ε_2 for a value of ε_3 which increases in steps of 0.02 from -0.1 in the top left plot to $+0.1$ in the bottom right plot. The increase in ε_1 is left to right first and then onto the lower row.

hand, for particular combinations of the applied strain, the bond polarity term can dominate and results in a positive sign of the PZCs. By contrast, in the LRM, the balance between these two contributions is lost inside the computational framework and the physical behaviour cannot be extracted in a meaningful way.

VI. LINEAR AND NON-LINEAR PIEZOELECTRIC COEFFICIENTS

To further investigate and ultimately quantify the non-linearities, we obtain the non-linear PZCs by fitting a third order polynomial to the DFT calculated values, after we impose conditions on the coefficients based on the cubic symmetry of the crystal. This leads to a reduced number of coefficients for the fitting equation

$$e'_{lm} = e_{lm} + \sum_{n=1}^3 e_{lnm} \varepsilon_n + \sum_{n \leq n'=1}^3 e_{lnn'm} \varepsilon_n \varepsilon_{n'} + \sum_{n \leq n' \leq n''=1}^3 e_{lnn'n''m} \varepsilon_n \varepsilon_{n'} \varepsilon_{n''}, \quad (8)$$

where again reduced indexes ($x=1$, $y=2$, $z=3$, $yz=4$, $xz=5$, $xy=6$) are used.

The numerical values obtained from the parameterization procedure are listed in Table I. For InAs, it was necessary to give more weight to the data points corresponding to smaller strains ($|\varepsilon_i| \leq 0.6$) in order to obtain a satisfactory fit. This is motivated by the fact that any errors in the DFT calculation appear to become larger as the applied strain is increased.

It is worth stressing that we refer to as zero order the constant value in the expansion (e_{lm} , equivalent to the bulk value) while linear (e_{lnm}), quadratic ($e_{lnn'm}$), and cubic coefficients

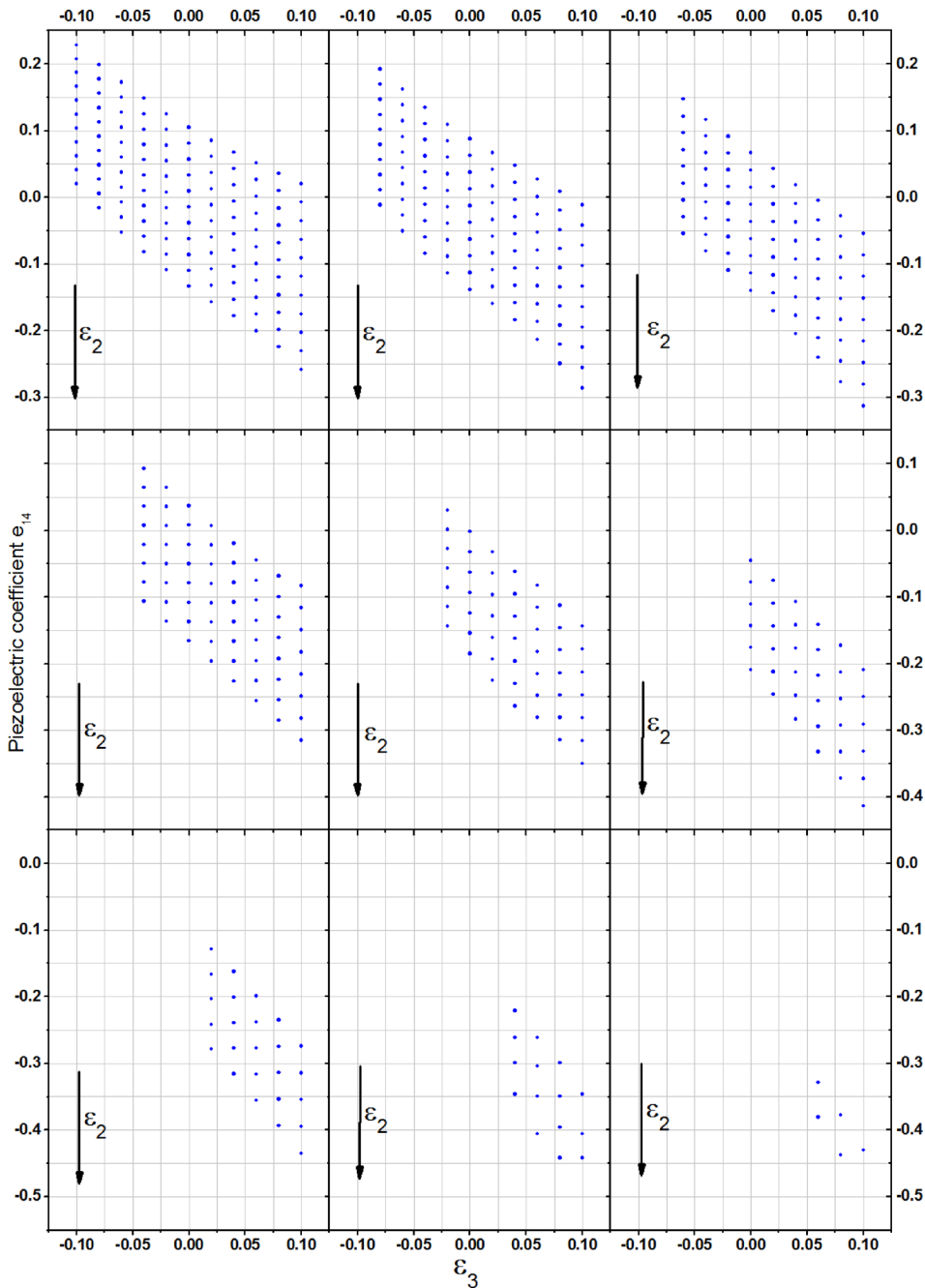


FIG. 2. Piezoelectric coefficient e_{14} (C/m^2) dependence on strain for InAs calculated from *ab-initio* DFT. The data display the dependence upon the strain components ϵ_1 and ϵ_2 for a value of ϵ_3 which increases in steps of 0.02 from -0.1 in the top left plot to $+0.1$ in the bottom right plot. The increase in ϵ_1 is left to right first and then onto the lower row.

($e_{lm'n'm}$) are terms coupled solely to the diagonal strain components. The polarization depends on the product of these terms times the shear components of the strain tensor, effectively making the PZ field quadratic in the strain even in the case where only the linear term in our expansion is used. This is different from the definition given by others^{12,13} where the linear term corresponds to the constant value of our expansion, while quadratic terms are the product of a term in the strain times a shear term, or the product of two shear terms.

A. Linear terms

Linear coefficients (e_{lm}) are coupled to strain components, such as ϵ_i with $i = 1, 3$. These coefficients are antisymmetric in nature. Both GaAs and InAs appear to have a smaller coefficient related to strain in the direction of

polarization compared with the ones linked to the plane orthogonal to the direction of polarization. For example, for polarization in the $i = 3$ direction (which for a (001) grown semiconductor would be the direction of growth), linked to the PZC e_{36} , the non-linearity is 3 times stronger for strain in the $i = 1$ and 2 (growth plane) directions compared to when the strain is in the direction of growth (Table II). Upon inspection of the data for the Kleinman parameter, we notice that the exact same dependence is observable, leading to the conclusion that this is predominantly an elastic effect due to the nature of the crystal structure.

In terms of magnitude, for both GaAs and InAs, strain coupled to the coefficient e_{114} in the range $\pm[10^{-2}, 10^{-1}]$ would contribute to the PZC third to second decimal place. The coefficient e_{124} would instead contribute to the PZC second to first decimal place in the same range.

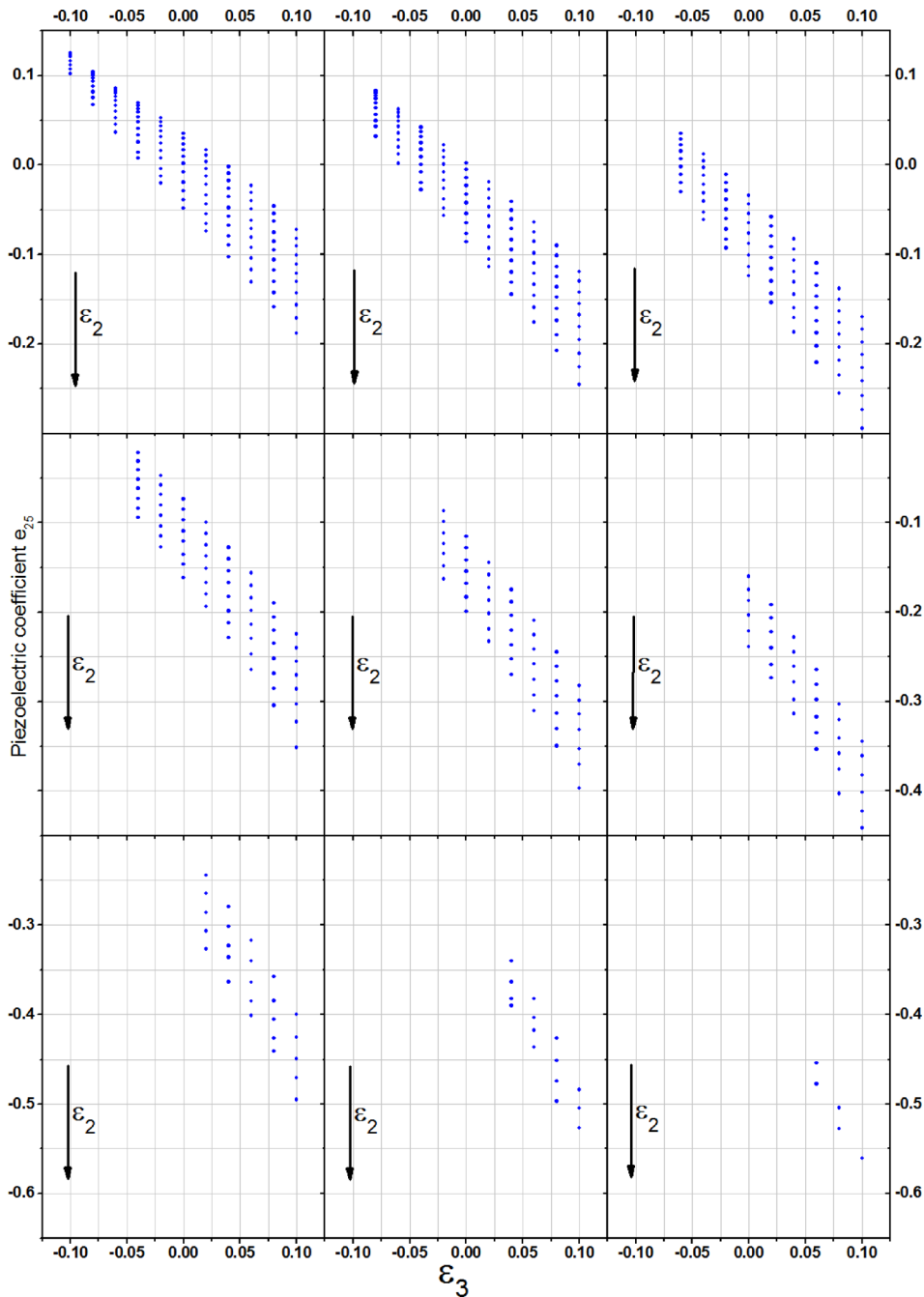


FIG. 3. Piezoelectric coefficient e_{25} (C/m^2) dependence on strain for GaAs calculated from *ab-initio* DFT. The data display the dependence upon the strain components ϵ_1 and ϵ_2 for a value of ϵ_3 which increases in steps of 0.02 from -0.1 in the top left plot to $+0.1$ in the bottom right plot. The increase in ϵ_1 is left to right first and then onto the lower row.

Hence, we conclude that linear terms are of sufficient magnitude to necessitate inclusion in any calculation of the PZ polarization in InAs and GaAs semiconductors.

B. Quadratic terms

Quadratic coefficients ($e_{lm'n'm}$) are coupled to strain components, such as $\epsilon_i\epsilon_j$ with $i, j = 1, 3$. Both these coefficients are symmetric if $i = j$ or antisymmetric if $i \neq j$.

GaAs and InAs appear to have different quadratic coefficients for different polarization and strain directions. This follows closely the differences already observed in the Kleinman parameters of both materials. In terms of magnitude, for both GaAs and InAs, strain coupled to the various quadratic coefficients in the range $\pm[10^{-2}, 10^{-1}]$ would contribute to the PZC fourth to second decimal place. Given that

the bulk coefficients are in the range $[10^{-1}, 10^{-2}] \text{ C}/\text{m}^2$ we conclude that quadratic terms are of sufficient magnitude to warrant inclusion in any calculation of the PZ polarization in InAs and GaAs semiconductors. Furthermore, the combination of linear and quadratic terms restores a fundamental asymmetry of the system related to the fact that compressive and tensile stress should produce neither symmetric nor antisymmetric effects.

C. Cubic terms

Cubic coefficients ($e_{lm'n'n'm}$) are coupled to strain terms, such as $\epsilon_i\epsilon_j\epsilon_k$ with $i, j, k = 1, 3$. These terms are antisymmetric in nature. Again GaAs and InAs appear to have different cubic coefficients for different polarization and strain directions. In particular, some are negligible for InAs but not for

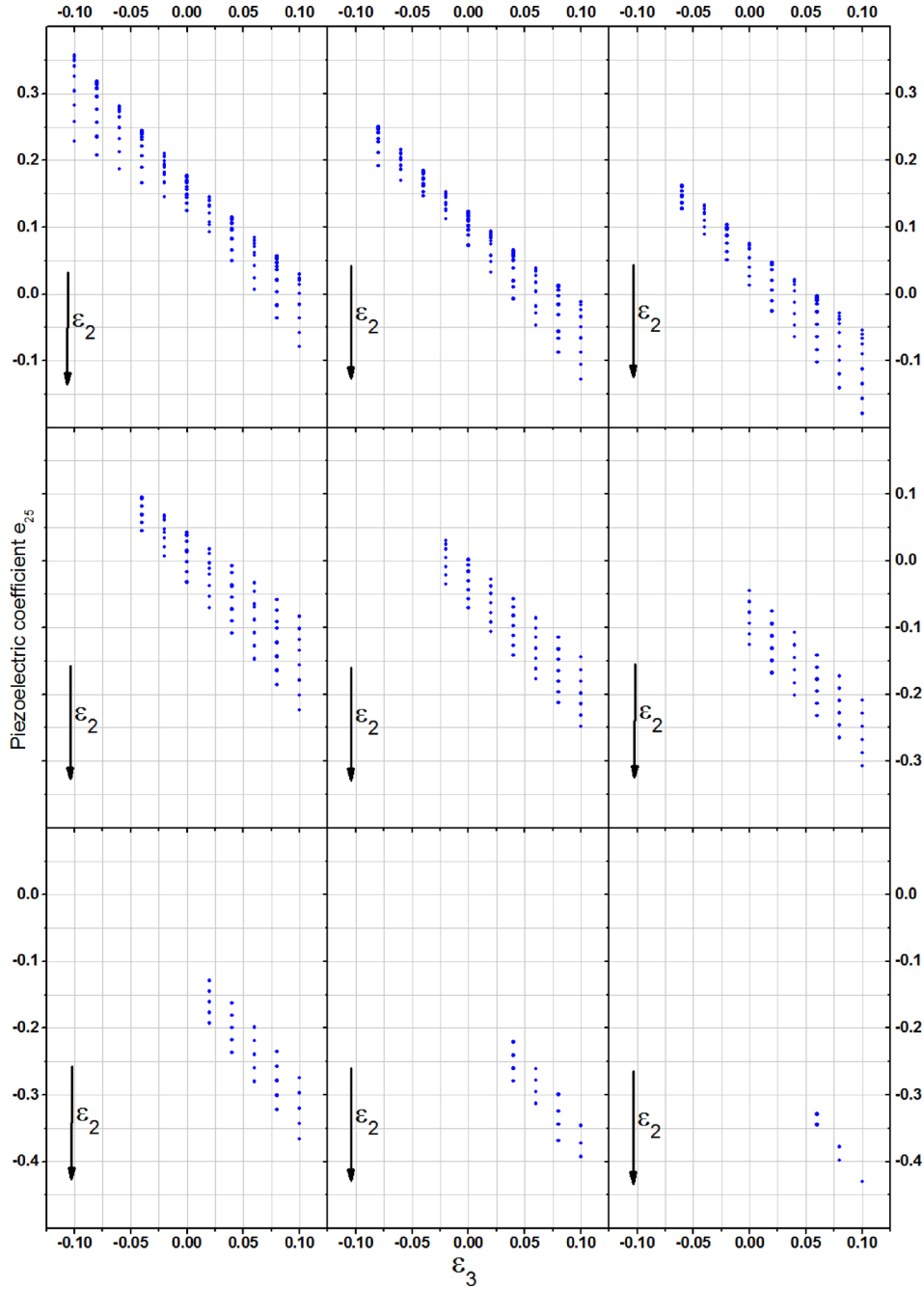


FIG. 4. Piezoelectric coefficient e_{25} (C/m^2) dependence on strain for InAs calculated from *ab-initio* DFT. The data display the dependence upon the strain components ϵ_1 and ϵ_2 for a value of ϵ_3 which increases in steps of 0.02 from -0.1 in the top left plot to $+0.1$ in the bottom right plot. The increase in ϵ_1 is left to right first and then onto the lower row.

GaAs. In terms of magnitude, for both GaAs and InAs, strain coupled to the largest cubic coefficients in the range $\pm[10^{-2}, 10^{-1}]$ would contribute to the PZC fifth to second decimal place. We conclude that cubic terms are of sufficient magnitude to recommend inclusion only in calculations of the PZ polarization involving InAs and GaAs semiconductors subject to particularly large strains (larger than 10%). For smaller strains the magnitude of the cubic correction is comparable to the error in the DFT calculations and can be therefore reasonably neglected.

VII. COMPARISON WITH LINEAR RESPONSE CALCULATIONS

The recent work by Beya-Wakata *et al.*¹³ presented a comprehensive study based on DFPT and linear response

theory of non-linear polarization in various III-V zinc blende semiconductors. The method used differs from ours as it relies entirely on *ab initio* calculation without any fitting parameters, which are instead used in our model (Z_H^*).

Their model considers an expansion of the polarization to linear and quadratic coefficients, which according to our definitions are the zero order and linear terms of Eq. (8), in the 6 components of the strain tensor

$$P = e_{14} \begin{pmatrix} \epsilon_4 \\ \epsilon_5 \\ \epsilon_6 \end{pmatrix} + e_{114} \begin{pmatrix} \epsilon_1 \epsilon_4 \\ \epsilon_2 \epsilon_5 \\ \epsilon_3 \epsilon_6 \end{pmatrix} + e_{124} \begin{pmatrix} \epsilon_4(\epsilon_2 + \epsilon_3) \\ \epsilon_5(\epsilon_1 + \epsilon_3) \\ \epsilon_6(\epsilon_2 + \epsilon_1) \end{pmatrix} + e_{156} \begin{pmatrix} \epsilon_5 \epsilon_6 \\ \epsilon_4 \epsilon_6 \\ \epsilon_4 \epsilon_5 \end{pmatrix}. \quad (9)$$

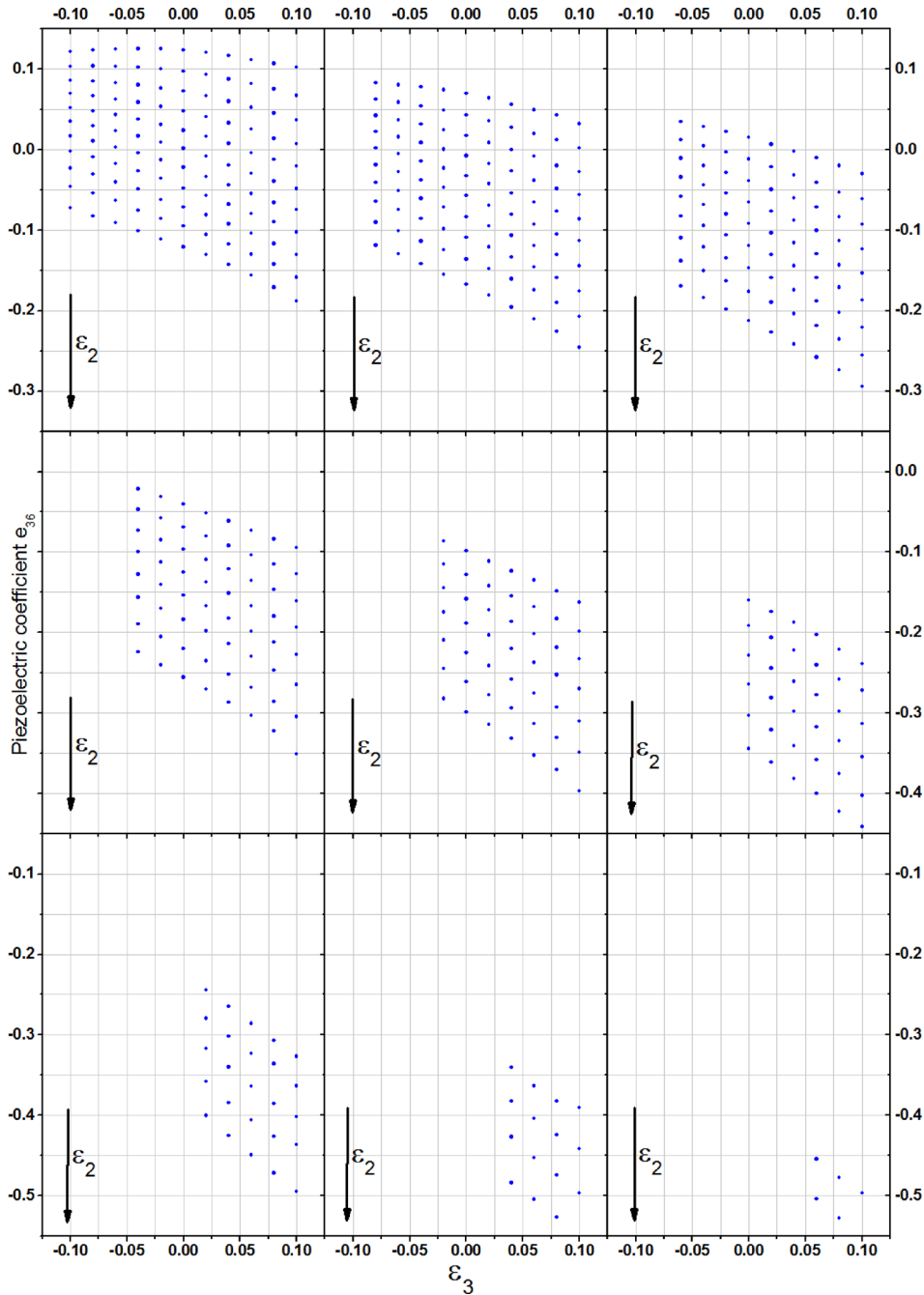


FIG. 5. Piezoelectric coefficient e_{36} (C/m^2) dependence on strain for InAs calculated from *ab-initio* DFT. The data display the dependence upon the strain components ϵ_1 and ϵ_2 for a value of ϵ_3 which increases in steps of 0.02 from -0.1 in the top left plot to $+0.1$ in the bottom right plot. The increase in ϵ_1 is left to right first and then onto the lower row.

As explained earlier in our model we neglected the e_{156} coefficient and therefore the quadratic dependence on the shear strain. Beya-Wakata *et al.*¹³ report values of e_{156} of $-0.7 \text{ C}/\text{m}^2$ and $0.2 \text{ C}/\text{m}^2$ for GaAs and InAs, respectively, which for the fixed shear strain of 0.02 used in our calculations would only affect the fifth decimal place. Though we do not incorporate such dependence in our model, one could in theory easily incorporate it by accepting their value of e_{156} .

To compare directly the 2 models, one needs to rewrite Eq. (9) using $\epsilon_4 = \epsilon_5 = \epsilon_6 = \gamma = 0.02$

$$P/\gamma = e_{14} + e_{114} \begin{pmatrix} \epsilon_1 \\ \epsilon_2 \\ \epsilon_3 \end{pmatrix} + e_{124} \begin{pmatrix} \epsilon_2 + \epsilon_3 \\ \epsilon_1 + \epsilon_3 \\ \epsilon_2 + \epsilon_1 \end{pmatrix} + e_{156}\gamma. \quad (10)$$

From this, it is clear that one of the major differences between the two models is that, while the non-linear response method introduces the small dependence on the quadratic shear strain, it neglects higher order contributions, such as the quadratic and cubic terms in the diagonal strain components. Our model instead obtains the latter via a fitting procedure of the DFT data. However, we can still compare the values of e_{14} , e_{114} , and e_{124} in the two models.

The values of e_{14} for GaAs and InAs in Beya-Wakata *et al.*¹³ are reported as $-0.238 \text{ C}/\text{m}^2$ and $-0.115 \text{ C}/\text{m}^2$, respectively, while in our model the values are fitted to exactly give the experimental values of $-0.16 \text{ C}/\text{m}^2$ and $-0.045 \text{ C}/\text{m}^2$. Beya-Wakata *et al.*¹³ point out that such experimental value could be affected by large errors due to interface polarization charges.²⁵ If this was verified, it would appear to cast doubts on our model parameters. However, the experimental values

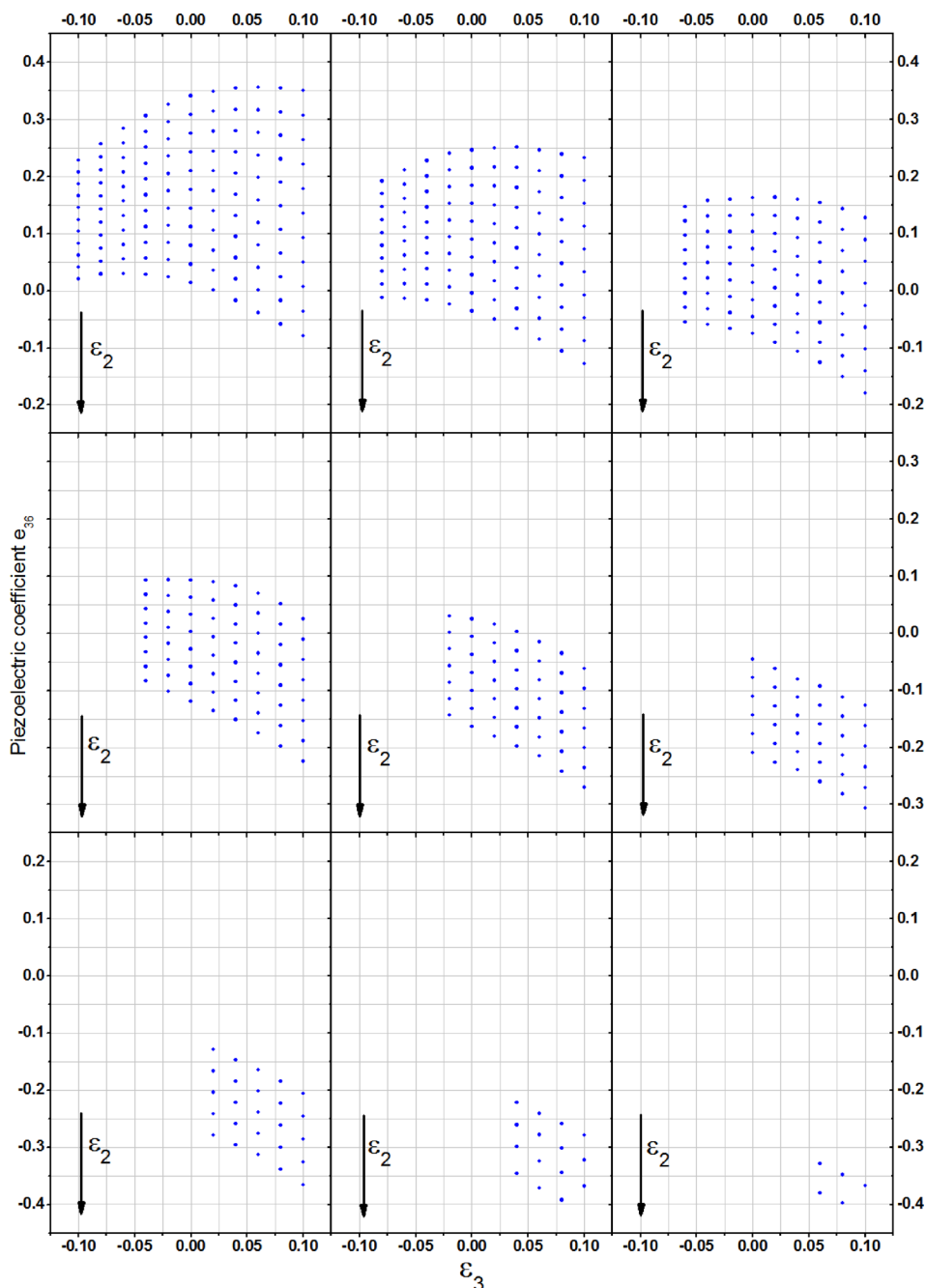


FIG. 6. Piezoelectric coefficient e_{36} (C/m^2) dependence on strain for InAs calculated from *ab-initio* DFT. The data display the dependence in the strain components ϵ_1 and ϵ_2 for a value of ϵ_3 which increase in steps of 0.02 from -0.1 in the top left plot to $+0.1$ in the bottom right plot. The increase in ϵ_1 is left to right first and then onto the lower row.

enter only one fitted quantity Z_{H}^* and our model could be easily recalibrated, whilst still maintaining the same non-linear behaviour as a function of strain.

There is instead a surprising quantitative agreement between the values of e_{114} for GaAs and InAs reported as $-0.4 \text{ C}/\text{m}^2$ and $-0.6 \text{ C}/\text{m}^2$ by Beya-Wakata *et al.*¹³ and $-0.666 \text{ C}/\text{m}^2$ and $-0.653 \text{ C}/\text{m}^2$ in our work. On the contrary, the values of e_{124} for GaAs and InAs reported as $-3.8 \text{ C}/\text{m}^2$ and $-4.1 \text{ C}/\text{m}^2$ by Beya-Wakata *et al.*¹³ and $-1.646 \text{ C}/\text{m}^2$ and $-1.617 \text{ C}/\text{m}^2$ in our work are different by over a factor of 2.

Particularly given the closeness of the values of e_{114} , there is no reasonable explanation for the discrepancy besides that maybe the inclusion of quadratic and maybe cubic terms in the Beya-Wakata *et al.*¹³ model could help reconciling in part such difference.

VIII. DISCUSSION

The two models discussed in this paper obviously produce very different results. We consider two critical cases for comparison: InAs pseudomorphically strained on GaAs (001) ($\epsilon_1 = \epsilon_2 = -0.7$, $\epsilon_3 = +0.7$, with a further shear component given by $\gamma = 0.02$), and on GaAs (111) ($\epsilon_1 = \epsilon_2 = \epsilon_3 = -0.223$, $\gamma = 0.268$). The Beya-Wakata *et al.*¹³ model predicts a polarization in the growth direction equal to $+0.069 \text{ C}/\text{m}^2$ for the (001) case and $+0.808 \text{ C}/\text{m}^2$ for the (111) case. We note that the linear term alone would in both cases predict a negative polarization. Our model too predicts a positive sign of the polarization, but of a much smaller magnitude: $+0.002 \text{ C}/\text{m}^2$ for the (001) and $+0.201 \text{ C}/\text{m}^2$ for the (111) case. This is a crucial difference that should be observable in experiment and could therefore help validating our model.

TABLE I. Linear and non-linear coefficients obtained from DFT data. For second and third order terms, the parameters are invariant upon cyclic permutation of the n indexes.

Coefficient	Condition on indexes	Degeneracy	GaAs	InAs
e_{lm}			-0.160	-0.045
e_{lmn}	$l = n$	$e_{114} = e_{225} = e_{336}$	-0.666	-0.653
	$l \neq n$	$e_{124} = e_{235} = e_{316}$ $n \leftrightarrow n'$	-1.646	-1.617
$e_{lmn'm}$	$l = n = n'$	$e_{1114} = e_{2225} = e_{3336}$	-0.669	-3.217
	$l = n \neq n'$	$e_{1124} = e_{1134} = e_{2215} = e_{2235} = e_{3316} = e_{3326}$	-2.694	-5.098
	$l \neq n = n'$	$e_{1224} = e_{1334} = e_{2115} = e_{2335} = e_{3116} = e_{3226}$	-1.019	1.590
	$l \neq n \neq n'$	$e_{1234} = e_{2135} = e_{3126}$ $n \leftrightarrow n' \leftrightarrow n''$	-5.636	-1.962
$e_{lmn'n'm}$	$l = n = n' = n''$	$e_{11114} = e_{22225} = e_{33336}$	-0.840	21.063
	$l = n = n' \neq n''$	$e_{11124} = e_{11134} = e_{22215} = e_{22235} = e_{33316} = e_{33326}$	-0.241	12.112
	$l \neq n = n' = n''$	$e_{12224} = e_{13334} = e_{21115} = e_{23335} = e_{31116} = e_{32226}$	-9.168	-15.072
	$l \neq n = n' \neq n''$	$e_{12234} = e_{21135} = e_{31126}$	-1.471	-7.450
	$n \neq n' \neq n''$	$e_{11234} = e_{21235} = e_{31236}$	-4.725	-4.909

At present, experimental data for zinc blende semiconductors appear to be inconclusive in validating either model, mostly due to the fact that it is not possible to completely isolate contributions arising from the piezoelectric field from those arising from other sources, such as interface charges and composition.

One element of validation for HM comes from the study of non-linearities in the PZ field of wurtzite III-N semiconductors, where together with 3 independent bulk PZCs there is also spontaneous polarization, therefore, providing potentially a more stringent test of validity compared to zinc blende crystals.⁸ In the case of InGaN QWs, comparison between experimental data and model data using HM's non-linear PZCs has certainly supported^{26,27} the validity of HM. However, no comparison has been published with the alternative non-linear PZCs obtained by Pedesseau *et al.*²⁸ within the LRM.

In terms of comparing HM and LRM models for zinc blende, one element that in our opinion casts doubts on the validity of LRM is that it predicts values of the first order coefficients (the linear terms) much larger (in absolute value) than the experimentally reported bulk values. To reconcile the LRM values with the experimental bulk values, one would have to assume the involuntary presence of compressive strain in excess of 10% when attempting to measure the bulk values. In HM instead the experimental bulk values are used to fit one of the dielectric properties. The difference between the models is that even in the limit of small strain the overall polarization is still much larger and negative in the LRM compared with both HM and the experimentally determined bulk values. While such difference could be the result of interface charges affecting the experimental

measurements, as Beya-Wakata *et al.*¹³ speculate, it seems too large for none to have been noticed over the many years of experimental work on PZ properties of semiconductors.

IX. THE EXAMPLE OF QUANTUM DOTS

In epitaxially grown InAs/GaAs QDs, the piezoelectric field is directly responsible for lifting the energy degeneracy of the otherwise indistinguishable p-type electron wavefunctions.²⁹⁻³¹ This is typically not the only cause of symmetry breaking, as in real structures structural (shape and crystal) asymmetries also play a vital part. We therefore discuss the differences between the piezoelectric potential distributions in the same nanostructure according to the conventional linear model (LM), the non-linear model (HM) of this work, and the non-linear model of Beya-Wakata *et al.*¹³ (LRM). The results are shown in Fig. 7. The InAs/GaAs QD used in the calculation is a square-based truncated pyramid with base width of 20 nm, height of 5 nm, and a top width of 10 nm. We are showing the PZ potential energy on a (001) plane intersecting the truncated pyramid at 1.5 nm, 2.5 nm and 3.5 nm from the base (30%, 50%, and 70% of the total height). There are significant differences between the models. For instance, the magnitude of the potential energy is certainly much larger for LRM compared with LM or HM near the top of the pyramid, while it appears comparable closer to the base. This difference near the top of the pyramid, where strains are typically larger,³² is the obvious result of the much larger values of e_{124} PZC. There are also differences between the spatial distribution of the potential energy between the linear and non-linear models. Closer to the top of the pyramid, the linear model appears to have a double structure on each lobe that in HM is spatially well separated, while it is not at all present in LRM. At the bottom of the pyramid, instead, it is the LM that predicts the largest magnitude and spatial extension of the potential. Furthermore, HM and LRM are comparable in magnitude but HM predicts a slightly larger field.

We further performed electronic structure calculations of the p-type orbital ($e1$ and $e2$ states) electron energies and wavefunctions using both the full 8-band and 14-band k-p formalism, including the kinetic part with the spin-orbit interaction, strain,

TABLE II. Comparison of the p-states electron wavefunctions energy difference (in meV) obtained by 8-band and 14-band k-p electronic structure calculations using different models for piezoelectricity: (a) Linear Model (LM), (b) Our Model (HM), and (c) Beya-Wakata Model¹³ (LRM).

k-p	Linear	HM (this work)	LRM (Beya Wakata) ¹³
14	18.0	10.1	7.8
8	18.2	10.3	7.9

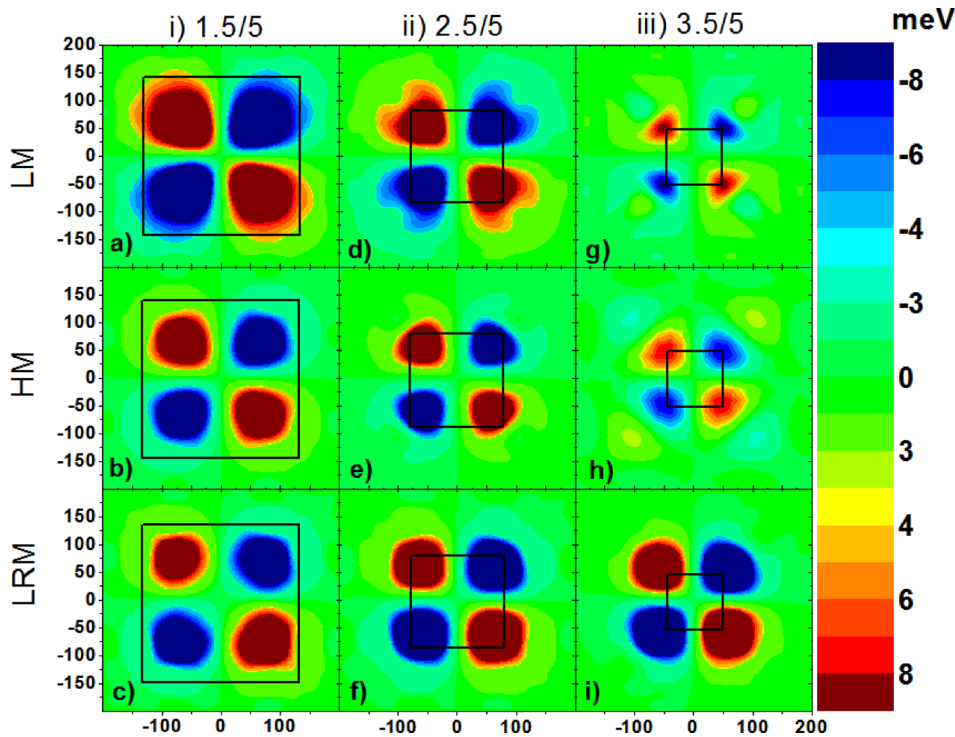


FIG. 7. Contour plots of piezoelectric potential energy of an InAs/GaAs Quantum Dot displayed columnwise on a (001) plane intersecting the pyramid at 1.5 nm, 2.5 nm, and 3.5 nm, respectively, from the base of the dot: (a) Linear Model (LM), (b) Our Model (HM), and (c) Beya-Wakata Model¹³ (LRM).

the interface Hamiltonian, as well as the strain-induced piezoelectric potential. The details of the method used can be found in Tomić and Vukmirović.³³ Both the 14-band and 8-band calculations yield the same result for the difference in energy of the p-state electron wavefunctions, within 0.2 meV (Table II). Since the electron wavefunctions tend to be spatially located at the bottom of the pyramid, the PZ potential calculated using the LM has the largest energy difference (18.1 ± 0.1 meV). HM and LRM give an energy difference of 10.2 ± 0.1 and 7.85 ± 0.05 meV, respectively. The difference between the HM and LRM models is significant. We also tested the influence of quadratic vs. cubic terms in HM and concluded that in truncated pyramidal QDs the quadratic terms are certainly very significant but the cubic terms only add a small positive correction of 0.1 meV. Hence in these particular structures, the strain is not sufficiently large to require inclusion of the cubic terms.

It is also noticeable that while both HM and LRM under particular strain combinations predict the possibility of positive values of the PZC, in neither of these calculations this appears to be the case. In Migliorato *et al.*,³⁰ it was proposed that the linear PZ field alone was able to account energy differences of the p-type electron wavefunctions in both InAs/GaAs and InGaAs QDs. The experimental values of these splitting were given in the same work as between 5 and 8 meV, close to the theoretical prediction. However, the experimental data also suggested that the [110] p-electron wavefunction should have been higher in energy compared with its $[\bar{1}\bar{1}0]$ counterpart. This could, in principle, be explained by the PZ field switching from negative to positive as a result of the strain in the nanostructure. However, in truncated pyramidal QDs not even non-linear models appear to predict a switch of the sign of the piezoelectric potential energy. One cannot exclude that some shapes or sizes of QDs other than the one used in this work could have strain large enough to be able to switch the polarization from

negative to positive. But at present we have to conclude that in experimental observations the degeneracy is mostly due to shape anisotropy counteracting and entirely reversing the effect of the piezoelectric field.

X. CONCLUSIONS

We have calculated the linear, quadratic, and cubic piezoelectric coefficients related to diagonal terms of the strain tensor for both GaAs and InAs zincblende crystals. We have assessed the magnitude of these extra terms and conclude that, while linear and quadratic terms are likely to necessitate inclusion even in the limit of small strain, cubic terms should only be included when the material undergoes significant (around 10%) strain.

Though currently synthesized nanostructures do not tend to exhibit such large strain, semiconductor materials are able to withstand high external pressure capable of compressing the wafer by 10% or more. Therefore, when measuring the electro-optical properties of semiconductor layers under external pressure one would necessarily need to use the cubic terms in order to model the resulting polarization and compare with the experimental data.

We tested whether in semiconductor InAs/GaAs truncated pyramidal Quantum Dots only quadratic or also cubic terms should be taken into account in electronic structure calculations and confirm that in such structures the strain is not large enough to necessitate inclusion of the cubic piezoelectric coefficients, but corrections due to the linear and quadratic terms (in the diagonal strain components) have a magnitude comparable to the conventional linear model.

¹R. M. Martin, *Phys. Rev. B* **5**, 1607 (1972).

²W. G. Cady, *Piezoelectricity* (McGraw-Hill, New York, 1946).

³S. Nakamura and G. Fasol, *The Blue Laser Diode: GaN Based Light Emitters and Lasers* (Springer-Verlag, Berlin, 1997).

- ⁴Z. L. Wang “Nano-piezotronics,” *Adv. Mater.* **19**, 889–992 (2007).
- ⁵R. S. Yang, Y. Qin, L. M. Dai, and Z. L. Wang, *Nat. Nanotechnol.* **4**, 34–39 (2009).
- ⁶S. Xu, Y. Qin, C. Xu, Y. G. Wei, R. S. Yang, and Z. L. Wang, *Nat. Nanotechnol.* **5**, 366 (2010).
- ⁷Z. L. Wang, *Sci. Am.* **298**, 82–87 (2008).
- ⁸J. Pal, G. Tse, V. Haxha, M. A. Migliorato, and S. Tomic, *Phys. Rev. B* **84**, 085211 (2011).
- ⁹L. C. Lew Yan Voon and M. Willatzen, *J. Appl. Phys.* **109**, 031101 (2011).
- ¹⁰H. Y. S. Al-Zahrani, J. Pal, and M. A. Migliorato, “Non-linear piezoelectricity in wurtzite ZnO semiconductors,” *Nano Energy* (published online).
- ¹¹M. A. Migliorato, D. Powell, A. G. Cullis, T. Hammerschmidt, and G. P. Srivastava, *Phys. Rev. B* **74**, 245332 (2006).
- ¹²G. Bester, X. Wu, D. Vanderbilt, and A. Zunger, *Phys. Rev. Lett.* **96**, 187602 (2006).
- ¹³A. Beya-Wakata, P.-Y. Prodhomme, and G. Bester, *Phys. Rev. B* **84**, 195207 (2011).
- ¹⁴W. A. Harrison, *Electronic Structure and Properties of Solids* (Dover Publications, Inc., New York, 1989).
- ¹⁵R. Garg, A. Hüe, V. Haxha, M. A. Migliorato, T. Hammerschmidt, and G. P. Srivastava, *Appl. Phys. Lett.* **95**, 041912 (2009).
- ¹⁶F. Bernardini and V. Fiorentini, *Appl. Phys. Lett.* **80**, 4145 (2002).
- ¹⁷N. Troullier and J. L. Martins, *Phys. Rev. B* **43**, 1993 (1991).
- ¹⁸J. P. Perdew and A. Zunger, *Phys. Rev. B* **23**, 5048 (1981).
- ¹⁹S. J. Clark, M. D. Segall, C. J. Pickard, P. J. Hasnip, M. J. Probert, K. Refson, and M. C. Payne, *Z. Kristallogr.* **220**(5–6), 567–570 (2005).
- ²⁰S.-H. Lee, J.-H. Kang, and M.-H. Kang, *J. Korean Phys. Soc.* **31**, 811 (1997).
- ²¹L. Kleinman, *Phys. Rev.* **128**, 2614 (1962).
- ²²M. V. Berry, *Proc. R. Soc. Lond. A* **392**, 45–57 (1984).
- ²³See supplementary material as <http://dx.doi.org/10.1063/1.4818798> for the Kleinman Vector and Bond Polarity as a function of strain in Figures 1–4 for InAs and GaAs. The plots display the dependence in the strain components ε_1 and ε_2 for a value of ε_3 which increases in steps of 0.02 from -0.1 in the top left plot to $+0.1$ in the bottom right plot. The increase in ε_1 is left to right first and then onto the lower row. Not all possible combinations of diagonal strains are shown as cubic symmetry implies invariance upon exchange of ε_1 , ε_2 , and ε_3 .
- ²⁴D. Powell, M. A. Migliorato, and A. G. Cullis, *Phys. Rev. B* **75**, 115202 (2007).
- ²⁵G. Arlt and P. Quadflieg, *Phys. Status Solidi B* **25**, 323 (1968).
- ²⁶B. G. Crutchley, I. P. Marko, J. Pal, M. A. Migliorato, and S. J. Sweeney, *Phys. Status Solidi B* **250**, 698–702 (2013).
- ²⁷T. Suski, S. P. Łepkowski, G. Staszczak, R. Czernecki, P. Perlin, and W. Bardyszewski, *J. Appl. Phys.* **112**, 053509 (2012).
- ²⁸L. Pedesseau, C. Katan, and J. Even, *Appl. Phys. Lett.* **100**, 031903 (2012).
- ²⁹M. A. Migliorato, D. Powell, S. L. Liew, A. G. Cullis, P. Navaretti, M. J. Steer, and M. Hopkinson, *J. Appl. Phys.* **96**, 5169–5172 (2004).
- ³⁰M. A. Migliorato, D. Powell, E. A. Zibik, L. R. Wilson, M. Fearn, J. H. Jefferson, M. J. Steer, M. Hopkinson, and A. G. Cullis, *Physica E (Amsterdam)* **26**, 436–440 (2005).
- ³¹G. Bester, A. Zunger, X. Wu, and D. Vanderbilt, *Phys. Rev. B* **74**, 081305(R) (2006).
- ³²V. Haxha, I. Drouzas, J. M. Ulloa, M. Bozkurt, P. M. Koenraad, D. J. Mowbray, H. Y. Liu, M. J. Steer, M. Hopkinson, and M. A. Migliorato, *Phys. Rev. B* **80**, 165334 (2009).
- ³³S. Tomic and N. Vukmirović, *J. Appl. Phys.* **110**, 053710 (2011).